Measurements of ggF and VBF of the Higgs boson in $H \rightarrow WW^{*} \rightarrow e\nu\mu\nu$ decays using $p\,p$ collisions at $\sqrt{s}$ = 13 TeV with the ATLAS detector

23.11.2021-24.11.2021

Anamika Aggarwal

Why HWW?

- Large Branching ratio
- Clean signal in leptonic decay mode

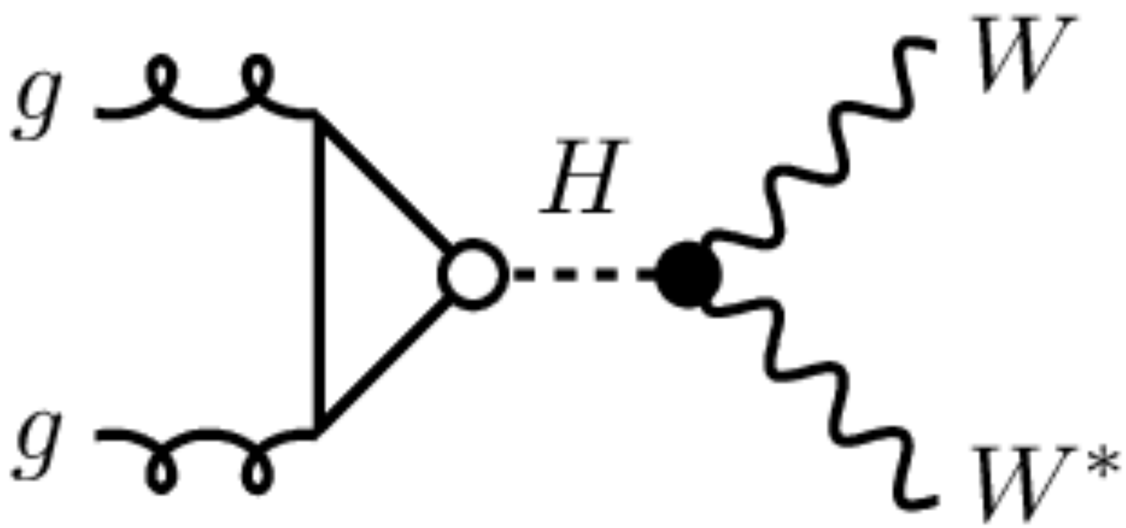

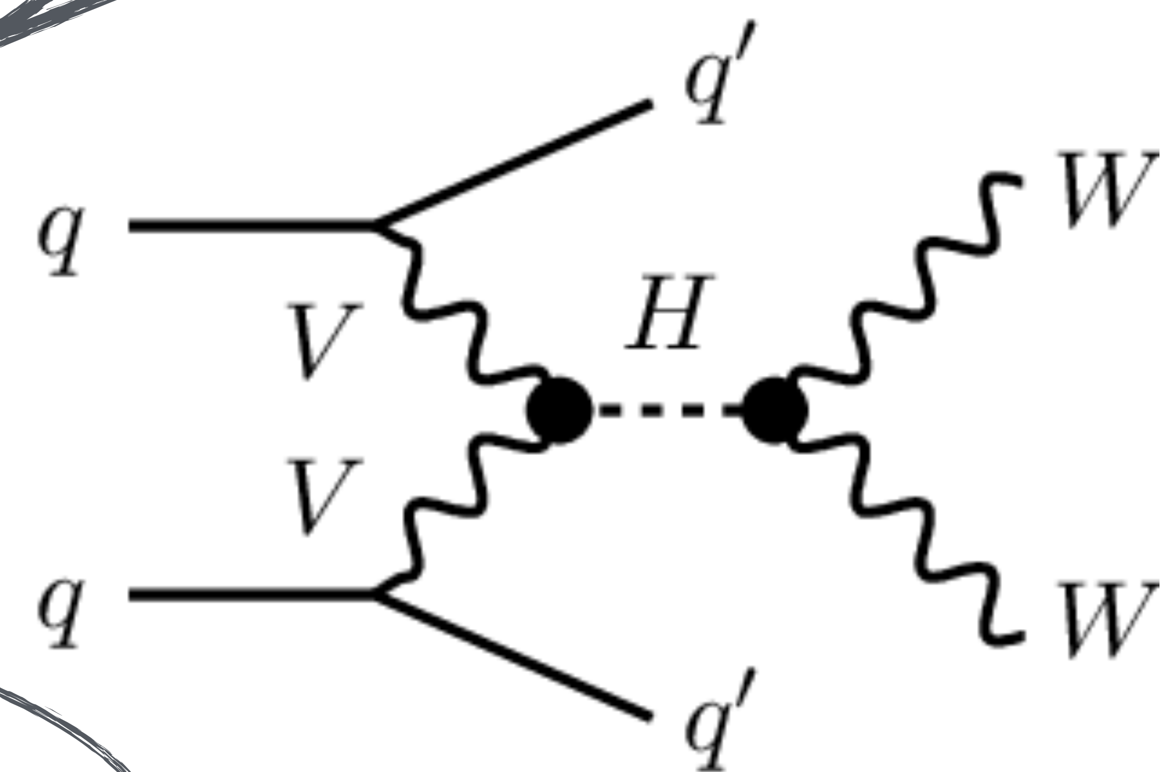

Mode and Channel

- H⇨WW*⇨$e\nu\mu\nu$ decay channel
- Different flavour channel

All the figures and tables are taken from ATLAS-CONF-2021-014

SIGNAL, BACKGROUNDS AND DATA

Signal

- ggF associated with 0 jet, 1 jet and ≥2 jet
- VBF associated with ≥2 jet

Data

- Full Run-2 Data
- 139 fb^{-1} Luminosity

Backgrounds

- Standard Model WW → Dedicated CRs
- $t\bar{t}$+Wt → Dedicated CRs
- Z/γ^*+jets → Dedicated CRs
- W+jets → Data-Driven Fake factor method for Mis-identified Lepton Estimation
- $V\gamma$ → Estimated from MC
- WZ/γ^*, ZZ → Estimated from MC
- VH signal → Fixed to SM predictions

MIS-IDENTIFIED LEPTON ESTIMATION

- Events with one or more mis-identified, or "fake", leptons, primarily from W+jets events.
- Not modelled reliably by simulation; estimated with a data-driven method.

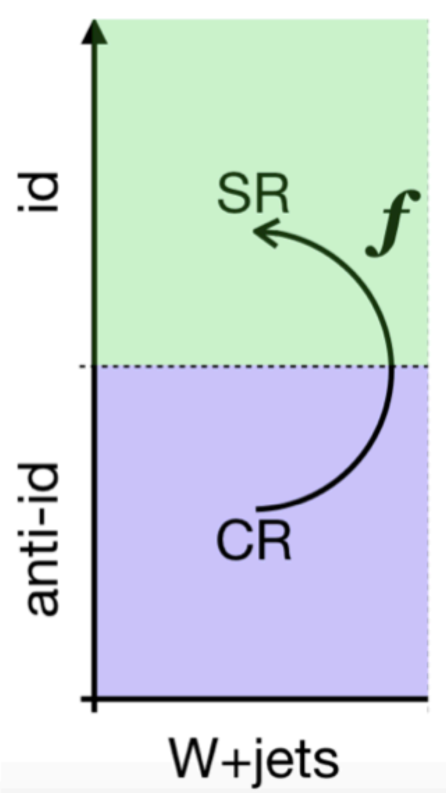

Extrapolation for 2-lepton final state:

$$N^{\text{id,id}}_{\geq 1\ \text{mis-id}} = f_e \cdot (N^{\text{anti-id,id}} - N^{\text{anti-id,id}}_{\text{prompt}}) + f_\mu \cdot (N^{\text{id,anti-id}} - N^{\text{id,anti-id}}_{\text{prompt}}) - f_e f_\mu \cdot (N^{\text{anti-id,anti-id}} - N^{\text{anti-id,anti-id}}_{\text{prompt}})$$

Last -term: account for double-fake events

SIGNAL REGIONS

<table>
<tr><th>Category</th><th>$N_{\text{jet},(p_T>30\text{ GeV})} = 0$ ggF</th><th>$N_{\text{jet},(p_T>30\text{ GeV})} = 1$ ggF</th><th>$N_{\text{jet},(p_T>30\text{ GeV})} \geq 2$ ggF</th><th>$N_{\text{jet},(p_T>30\text{ GeV})} \geq 2$ VBF</th></tr>
<tr><td rowspan="2">Preselection</td><td colspan="4">Two isolated, different-flavour leptons ($\ell = e, \mu$) with opposite charge
$p_T^{\text{lead}} > 22$ GeV , $p_T^{\text{sublead}} > 15$ GeV
$m_{\ell\ell} > 10$ GeV</td></tr>
<tr><td colspan="3">$p_T^{\text{miss}} > 20$ GeV</td><td></td></tr>
<tr><td rowspan="3">Background rejection</td><td colspan="4">$N_{b\text{-jet},(p_T>20\text{ GeV})} = 0$</td></tr>
<tr><td rowspan="2">$\Delta\phi_{\ell\ell,E_T^{\text{miss}}} > \pi/2$
$p_T^{\ell\ell} > 30$ GeV</td><td colspan="3">$m_{\tau\tau} < m_Z - 25$ GeV</td></tr>
<tr><td>$\max\left(m_T^{\ell}\right) > 50$ GeV</td><td colspan="2"></td></tr>
<tr><td rowspan="3">$H \to WW^* \to e\nu\mu\nu$
topology</td><td colspan="3">$m_{\ell\ell} < 55$ GeV
$\Delta\phi_{\ell\ell} < 1.8$</td><td rowspan="3">central jet veto
outside lepton veto
$m_{jj} > 120$ GeV</td></tr>
<tr><td colspan="2" rowspan="2"></td><td>fail central jet veto
or
fail outside lepton veto</td></tr>
<tr><td>$|m_{jj} - 85| > 15$ GeV
or
$\Delta y_{jj} > 1.2$</td></tr>
<tr><td>Discriminant variable</td><td colspan="3">m_T</td><td>DNN</td></tr>
</table>

ggF: 3 signal regions based on the Njet category.
VBF: only one signal region.

CONTROL REGIONS

- 3 control regions corresponding to 3 major backgrounds in each Njet category in ggF case
- only 2 control regions in VBF case.

CR	$N_{\text{jet},(p_T>30\text{ GeV})}=0$ ggF	$N_{\text{jet},(p_T>30\text{ GeV})}=1$ ggF	$N_{\text{jet},(p_T>30\text{ GeV})}\geq 2$ ggF	$N_{\text{jet},(p_T>30\text{ GeV})}\geq 2$ VBF
$qq\to WW$	$N_{b\text{-jet},(p_T>20\text{ GeV})}=0$			
	$55<m_{\ell\ell}<110$ GeV	$m_{\ell\ell}>80$ GeV		
	$\Delta\phi_{\ell\ell}<2.6$	$\lvert m_{\tau\tau}-m_Z\rvert>25$ GeV $\max(m_T^{\ell})>50$ GeV	$m_{\tau\tau}<m_Z-25$ GeV $m_{T2}>165$ GeV	
			fail central jet veto or fail outside lepton veto	
			$\lvert m_{jj}-85\rvert>15$ GeV or $\Delta y_{jj}>1.2$	
$t\bar{t}/Wt$	$N_{b\text{-jet},(20\text{ GeV}<p_T<30\text{ GeV})}>0$	$N_{b\text{-jet},(p_T>30\text{ GeV})}=1$ $N_{b\text{-jet},(20\text{ GeV}<p_T<30\text{ GeV})}=0$	$N_{b\text{-jet},(p_T>20\text{ GeV})}=0$	$N_{b\text{-jet},(p_T>20\text{ GeV})}=1$
	$\Delta\phi(\ell\ell,E_T^{\text{miss}})>\pi/2$ $p_T^{\ell\ell}>30$ GeV $\Delta\phi_{\ell\ell}<2.8$	$m_{\tau\tau}<m_Z-25$ GeV		
		$\max(m_T^{\ell})>50$ GeV	$m_{\ell\ell}>80$ GeV $\Delta\phi_{\ell\ell}<1.8$ $m_{T2}<165$ GeV	
			fail central jet veto or fail outside lepton veto	central jet veto outside lepton veto
			$\lvert m_{jj}-85\rvert>15$ GeV or $\Delta y_{jj}>1.2$	
Z/γ^*	$N_{b\text{-jet},(p_T>20\text{ GeV})}=0$			
	$m_{\ell\ell}<80$ GeV no p_T^{miss} requirement		$m_{\ell\ell}<55$ GeV	$m_{\ell\ell}<70$ GeV
	$\Delta\phi_{\ell\ell}>2.8$	$m_{\tau\tau}>m_Z-25$ GeV		$\lvert m_{\tau\tau}-m_Z\rvert\leq 25$ GeV central jet veto outside lepton veto
			fail central jet veto or fail outside lepton veto	
			$\lvert m_{jj}-85\rvert>15$ GeV or $\Delta y_{jj}>1.2$	

UNCERTAINTIES

Experimental Uncertainties

[Standard set of four-vector and scale-factor uncertainties, following recommendations from CP groups]

- Trigger (efficiency)
- Electron (reconstruction, ID, energy scale, resolution, isolation)
- Muon (reconstruction, ID, momentum scale, resolution, TTVA, isolation)
- Jets (JES, JER, flavour tagging)
- MET (Soft term, jet track scale)
- Pileup, Lumi
- Fake Factor uncertainties
- Mis-ID (stats, EW subtraction, flavour composition)

Theory Uncertainties

[Considered on all the main backgrounds: WW, top, Z+jets and both ggF and VBF signals]

- qqWW: Matching, PS, PDF, QCD scale
- ggWW: QCD scale
- $t\bar{t}$: Matching, PS, PDF, QCD scale, ISR/FSR
- Wt: Matching, PS, PDF, QCD scale, ISR/FSR, interference
- Z+jets: Generator, PDF, QCD scale
- ggF: QCD scale, PS/UE (P8 vs H7), PDF
- VBF: QCD scale, PS/UE (P8 vs H7), PDF, matching

GGF

Results derived with simultaneous maximum likelihood fit using m_T as the discriminant variable.

$$m_{\mathrm{T}} = \sqrt{\left(E_{\mathrm{T}}^{\ell\ell} + E_{\mathrm{T}}^{\mathrm{miss}}\right)^2 - \left|\boldsymbol{p}_{\mathrm{T}}^{\ell\ell} + \boldsymbol{E}_{\mathrm{T}}^{\mathrm{miss}}\right|^2} \quad \text{where } E_{\mathrm{T}}^{\ell\ell} = \sqrt{|\boldsymbol{p}_{\mathrm{T}}^{\ell\ell}|^2 + m_{\ell\ell}^2}$$

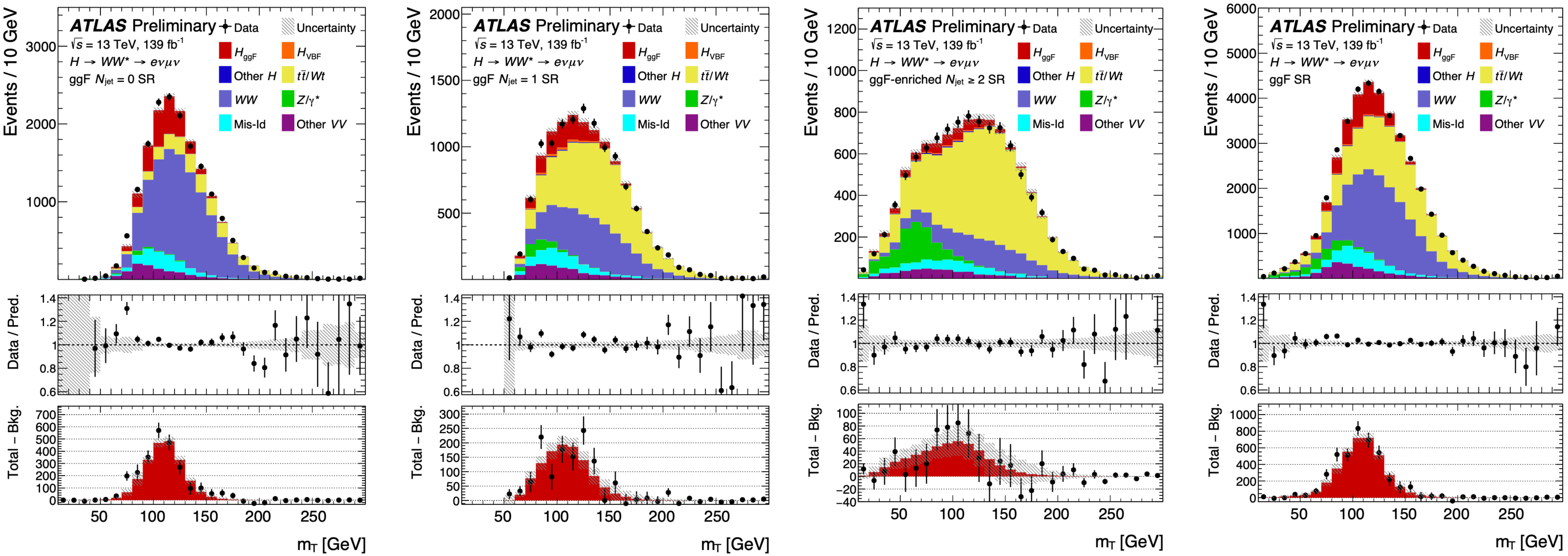

$$\sigma_{\mathrm{ggF}} \cdot \mathcal{B}_{H\to WW^*} = 12.4 \pm 1.5 \text{ pb}$$
$$= 12.4 \pm 0.6 \text{ (stat.)} \pm 0.9 \text{ (exp syst.)} {}^{+0.7}_{-0.6} \text{ (sig theo.)} \pm 1.0 \text{ (bkg theo.) pb}$$

$$\mu_{\mathrm{ggF}} = 1.20 {}^{+0.16}_{-0.15}$$
$$= 1.20 \pm 0.05 \text{ (stat.)} {}^{+0.09}_{-0.08} \text{ (exp syst.)} {}^{+0.10}_{-0.08} \text{ (sig theo.)} {}^{+0.12}_{-0.11} \text{ (bkg theo.)}$$

VBF

- Results derived with simultaneous maximum likelihood fit using new multi-variate discriminant using a Deep Neural Network (DNN)
- DNN is applied in the SR that uses 15 discriminant variables:

$$\Delta\phi_{\ell\ell}, m_{\ell\ell}, m_{\mathrm{T}}, \Delta y_{jj}, m_{jj}, p_{\mathrm{T}}^{\mathrm{tot}}, \sum_{\ell} C_{\ell},$$
$$m_{\ell_1 j_1}, m_{\ell_1 j_2}, m_{\ell_2 j_1}, m_{\ell_2 j_2},$$
$$p_{\mathrm{T}}^{\mathrm{jet}_1}, p_{\mathrm{T}}^{\mathrm{jet}_2}, p_{\mathrm{T}}^{\mathrm{jet}_3}, \text{ and } \mathrm{E}_{\mathrm{T}}^{\mathrm{miss}} \text{ significance}$$

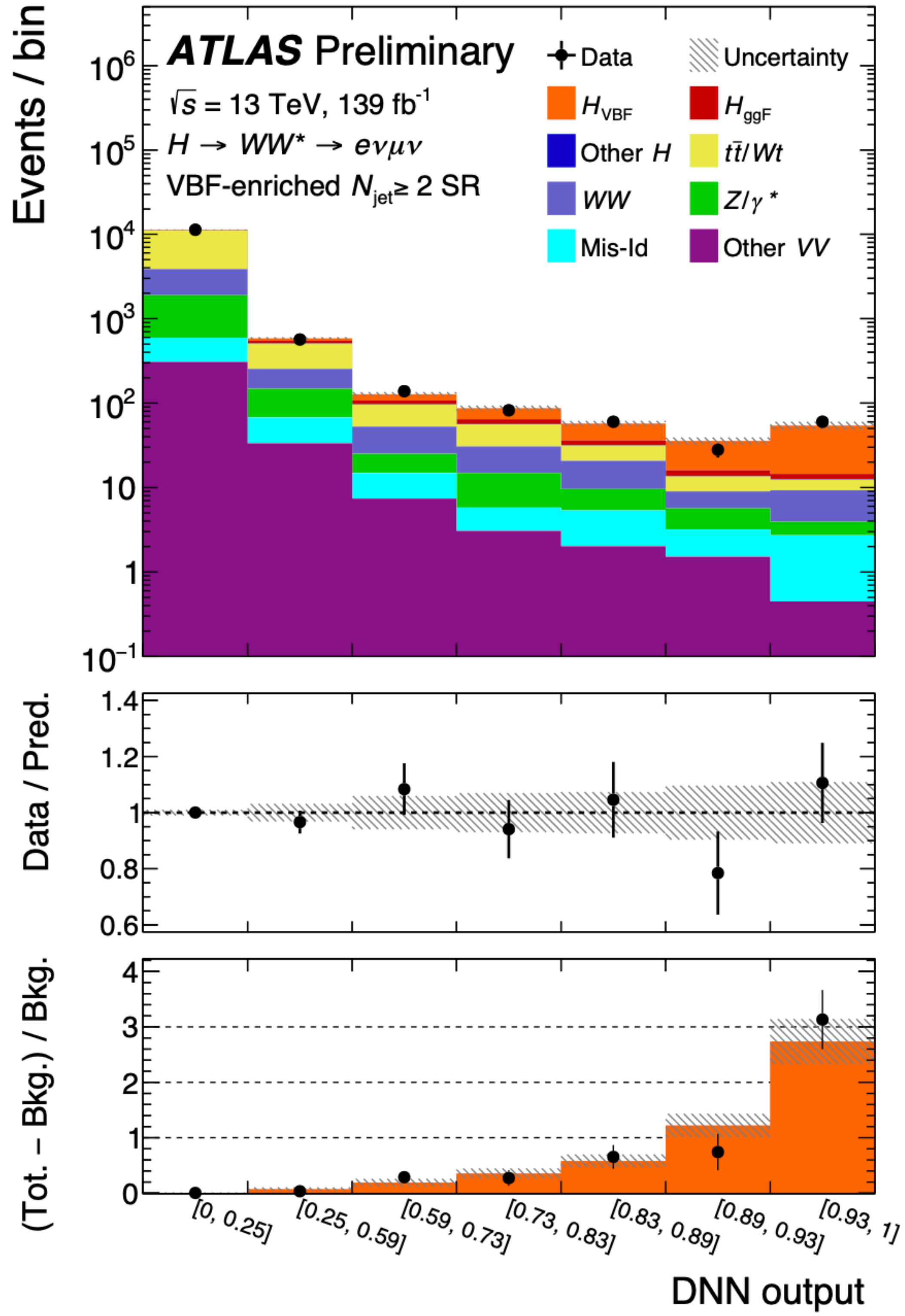

$$\sigma_{\mathrm{VBF}} \cdot \mathcal{B}_{H\to WW^*} = 0.79\,^{+0.19}_{-0.16}\ \mathrm{pb}$$
$$= 0.79\,^{+0.11}_{-0.10}\ (\mathrm{stat.})\ ^{+0.06}_{-0.05}\ (\mathrm{exp\ syst.})\ ^{+0.13}_{-0.09}\ (\mathrm{sig\ theo.})\ ^{+0.08}_{-0.06}\ (\mathrm{bkg\ theo.})\ \mathrm{pb}$$

$$\mu_{\mathrm{VBF}} = 0.99\,^{+0.24}_{-0.20}$$
$$= 0.99\,^{+0.13}_{-0.12}\ (\mathrm{stat.})\ ^{+0.07}_{-0.06}\ (\mathrm{exp\ syst.})\ ^{+0.17}_{-0.12}\ (\mathrm{sig\ theo.})\ ^{+0.10}_{-0.08}\ (\mathrm{bkg\ theo.})$$

STXS

- Cross section measurements are also conducted in the Stage-1.2 STXS category scheme.
- The STXS categories have been defined using the truth record of the simulated samples.
- After merging certain regions to ensure sensitivity for all the measured parameters, a total of 11 fiducial cross sections in different STXS categories are measured.
- 6 categories for ggH production and 5 for electroweak qqH production.

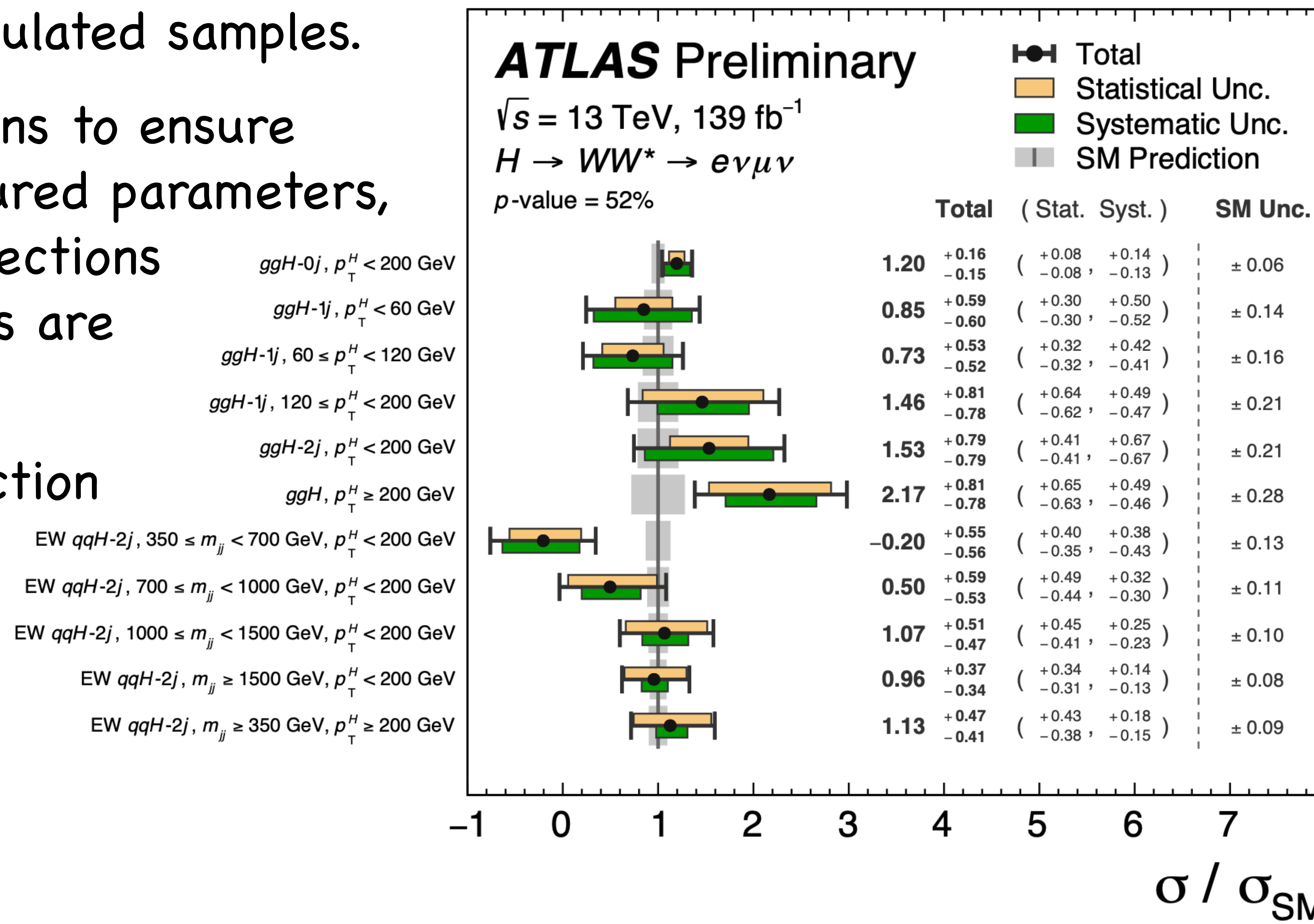

BREAKDOWN OF THE MAIN CONTRIBUTIONS TO THE TOTAL UNCERTAINTY

- Both measurements are dominated by systematic uncertainties.
- For the ggF measurement, uncertainties from both experimental and theoretical sources are comparable.
- For the VBF measurement, signal theory uncertainties make up the largest contribution.

Source	$\frac{\Delta\sigma_{\text{ggF}}\cdot\mathcal{B}_{H\to WW^*}}{\sigma_{\text{ggF}}\cdot\mathcal{B}_{H\to WW^*}}$ [%]	$\frac{\Delta\sigma_{\text{VBF}}\cdot\mathcal{B}_{H\to WW^*}}{\sigma_{\text{VBF}}\cdot\mathcal{B}_{H\to WW^*}}$ [%]
Data statistical uncertainties	5	13
Total systematic uncertainties	11	18
MC statistical uncertainties	4	3.2
Experimental uncertainties	6	7
Flavour Tagging	2.4	0.9
Jet energy scale	1.4	3.3
Jet energy resolution	2.3	1.9
$E_{\text{T}}^{\text{miss}}$	1.9	5
Muons	2.1	0.7
Electrons	1.5	0.3
Fake factors	2.4	1.0
Pile-up	2.4	1.3
Luminosity	2.0	2.1
Theoretical uncertainties	8	16
ggF	5	4
VBF	0.7	13
Top	4	5
$Z\tau\tau$	2.0	2.1
WW	4	5
Other VV	3	1.2
Background normalisations	5	5
WW	3.1	0.5
Top	2.4	2.2
$Z\tau\tau$	3.1	4
TOTAL	12	22

CONCLUSION

- ggF and VBF Higgs boson production modes are measured in the $H \to WW^* \to e\nu\mu\nu$ decay channel.
- ggF and VBF cross sections times the $H \to WW$ branching ratio are measured to be 12.4 ± 1.5 pb and 0.79 $^{+0.19}_{-0.16}$ pb, respectively, in agreement with the Standard Model predictions of 10.4 ± 0.6 pb and 0.81 ± 0.02 pb, respectively.
- Higgs boson production in the $H \to WW^*$ decay channel is further characterised through measurements of the Simplified Template Cross Sections in a total of 11 STXS categories.
- All the results are compatible with the Standard Model predictions with a p-value of 52%.

BACKUP

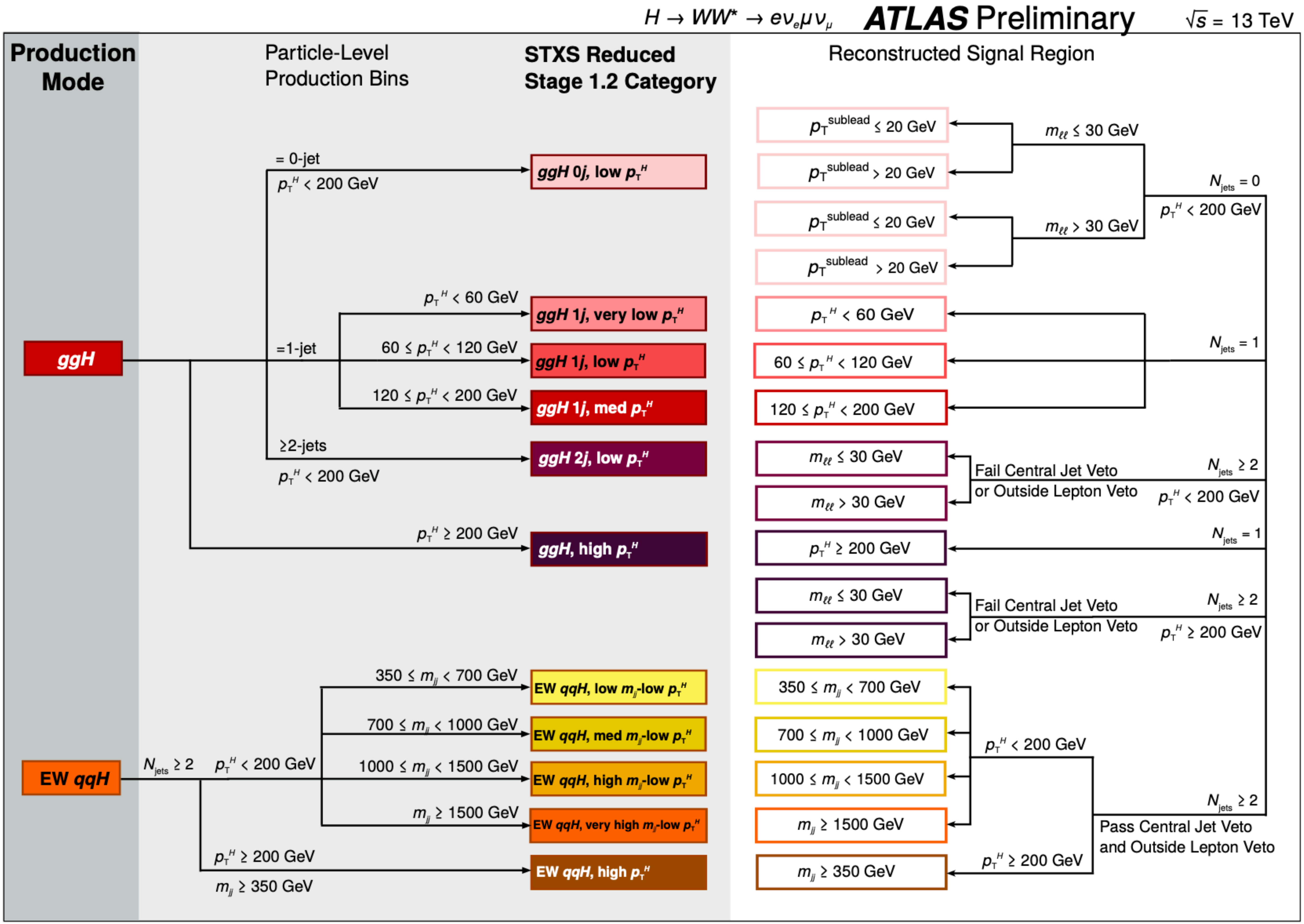

$H \to WW^* \to e\nu_e\mu\nu_\mu$ ATLAS Preliminary $\sqrt{s}$ = 13 TeV
Production Mode
Particle-Level Production Bins
STXS Reduced Stage 1.2 Category
Reconstructed Signal Region
ggH
EW qqH
= 0-jet
p_T^H < 200 GeV
=1-jet
p_T^H < 60 GeV
60 ≤ p_T^H < 120 GeV
120 ≤ p_T^H < 200 GeV
≥2-jets
p_T^H < 200 GeV
p_T^H ≥ 200 GeV
ggH 0j, low p_T^H
ggH 1j, very low p_T^H
ggH 1j, low p_T^H
ggH 1j, med p_T^H
ggH 2j, low p_T^H
ggH, high p_T^H
N_{jets} ≥ 2
p_T^H < 200 GeV
350 ≤ m_{jj} < 700 GeV
700 ≤ m_{jj} < 1000 GeV
1000 ≤ m_{jj} < 1500 GeV
m_{jj} ≥ 1500 GeV
p_T^H ≥ 200 GeV
m_{jj} ≥ 350 GeV
EW qqH, low m_{jj}-low p_T^H
EW qqH, med m_{jj}-low p_T^H
EW qqH, high m_{jj}-low p_T^H
EW qqH, very high m_{jj}-low p_T^H
EW qqH, high p_T^H
$p_T^{sublead}$ ≤ 20 GeV
$p_T^{sublead}$ > 20 GeV
$p_T^{sublead}$ ≤ 20 GeV
$p_T^{sublead}$ > 20 GeV
$m_{\ell\ell}$ ≤ 30 GeV
$m_{\ell\ell}$ > 30 GeV
N_{jets} = 0
p_T^H < 200 GeV
p_T^H < 60 GeV
60 ≤ p_T^H < 120 GeV
120 ≤ p_T^H < 200 GeV
N_{jets} = 1
$m_{\ell\ell}$ ≤ 30 GeV
$m_{\ell\ell}$ > 30 GeV
Fail Central Jet Veto
or Outside Lepton Veto
N_{jets} ≥ 2
p_T^H < 200 GeV
p_T^H ≥ 200 GeV
N_{jets} = 1
$m_{\ell\ell}$ ≤ 30 GeV
$m_{\ell\ell}$ > 30 GeV
Fail Central Jet Veto
or Outside Lepton Veto
N_{jets} ≥ 2
p_T^H ≥ 200 GeV
350 ≤ m_{jj} < 700 GeV
700 ≤ m_{jj} < 1000 GeV
1000 ≤ m_{jj} < 1500 GeV
m_{jj} ≥ 1500 GeV
m_{jj} ≥ 350 GeV
p_T^H < 200 GeV
p_T^H ≥ 200 GeV
N_{jets} ≥ 2
Pass Central Jet Veto
and Outside Lepton Veto

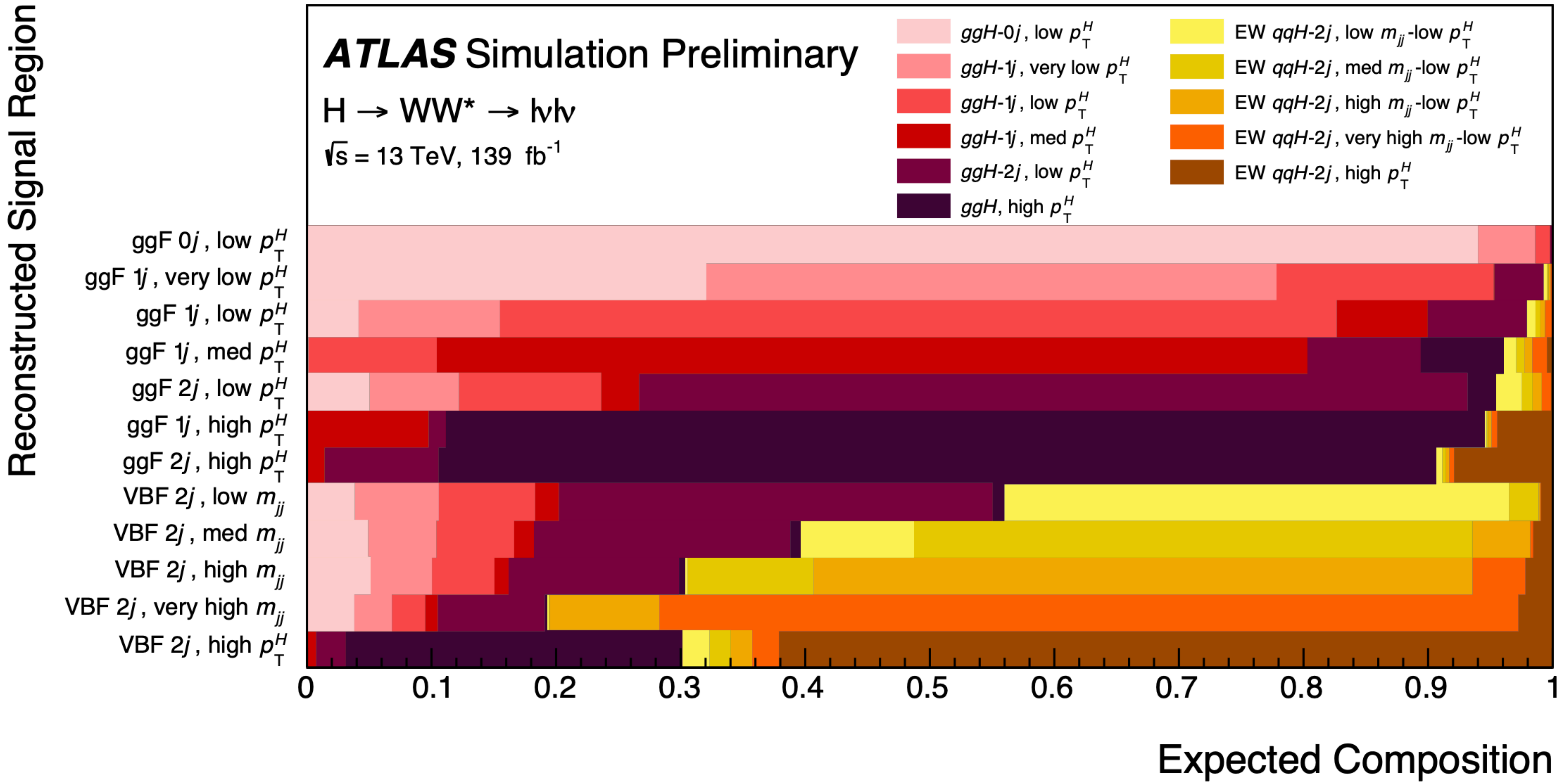

ATLAS Simulation Preliminary
H → WW* → lνlν
√s = 13 TeV, 139 fb-1
ggH-0j, low p_T^H
ggH-1j, very low p_T^H
ggH-1j, low p_T^H
ggH-1j, med p_T^H
ggH-2j, low p_T^H
ggH, high p_T^H
EW qqH-2j, low m_{jj}-low p_T^H
EW qqH-2j, med m_{jj}-low p_T^H
EW qqH-2j, high m_{jj}-low p_T^H
EW qqH-2j, very high m_{jj}-low p_T^H
EW qqH-2j, high p_T^H
Reconstructed Signal Region
ggF 0j, low p_T^H
ggF 1j, very low p_T^H
ggF 1j, low p_T^H
ggF 1j, med p_T^H
ggF 2j, low p_T^H
ggF 1j, high p_T^H
ggF 2j, high p_T^H
VBF 2j, low m_{jj}
VBF 2j, med m_{jj}
VBF 2j, high m_{jj}
VBF 2j, very high m_{jj}
VBF 2j, high p_T^H
0
0.1
0.2
0.3
0.4
0.5
0.6
0.7
0.8
0.9
1
Expected Composition